

Technical note

Hybrid energy converter based on swirling combustion chambers: the hydrocarbon feeding analysis

Angelo Minotti *

School of Aerospace Engineering, University of Rome “La Sapienza”, Via Salaria 851, Rome 00138, Italy

* **Correspondence:** Email: angelo.minotti@uniroma1.it; Tel: +39-328-289-1745.

Abstract: This manuscript reports the latest investigations about a miniaturized hybrid energy power source, compatible with thermal/electrical conversion, by a thermo-photovoltaic cell, and potentially useful for civil and space applications. The converter is a thermally-conductive emitting parallelepiped element and the basic idea is to heat up its emitting surfaces by means of combustion, occurred in swirling chambers, integrated inside the device, and/or by the sun, which may work simultaneously or alternatively to the combustion. The current upgrades consist in examining whether the device might fulfill specific design constraints, adopting hydrocarbons-feeding. Previous papers, published by the author, demonstrate the hydrogen-feeding effectiveness. The project's constraints are: 1) emitting surface dimensions fixed to 30×30 mm, 2) surface peak temperature $T > 1000$ K and the relative $\Delta T < 100$ K (during the combustion mode), 3) the highest possible delivered power to the ambient, and 4) thermal efficiency greater than 20% when works with solar energy. To this end, a 5 connected swirling chambers configuration (3 mm of diameter), with 500 W of injected chemical power, stoichiometric conditions and detailed chemistry, has been adopted. Reactive numerical simulations show that the stiff methane chemical structure obliges to increase the operating pressure, up to 10 atm, and to add hydrogen, to the methane fuel injection, in order to obtain stable combustion and efficient energy conversion.

Keywords: meso-combustor; hybrid energy-converter; methane-hydrogen/air combustion; whirl flow; fluid-structure interaction; computational fluid dynamics; detailed chemistry

1. Introduction

This manuscript is the progress of two previous works, carried out by the author [1,2], that come from the “EU-FP7-HRC-Power” project [3,4].

The goal of that European project is to design a novel energy device, able to overcome the high level of unused capacity and the high variability of the renewable sources over time (the intermittent nature leads to low capacity factors, low flexibility and high amortization costs).

To this end, a hybrid energy system, which adopts solar energy and/or chemical energy, has been defined; this kind of hybridization is able to provide reliable and continuous base-load power, as well as peak-load power.

Moreover, the project imposed the constraint of a miniaturized device, in order to enlarge its fields of application (i.e. smart buildings, mobiles, pc, satellites, space propulsion, etc.), and to allow different configurations (single and/or cluster operability).

The basic idea consists in integrating micro-swirling combustion chambers inside a parallelepiped brick, which is characterized by emitting surfaces that release heat power to be finally converted into electrical energy by a thermophotovoltaic cell (TPV).

Surfaces are heated up by the sun and/or by hot gases, produced during the combustion occurred in the micro-swirling chambers integrated inside the device.

The swirling chambers are adopted to permit efficient combustion in miniaturized devices (swirling motion increases the residence time), without the necessity of catalytic deposition on the internal walls (a procedure as expensive and difficult as the device is shrunk).

No works like this, apart from what it has been carried out by the author, are available; therefore, it is not possible to provide more comparative data than what it has already been done in [2], where a 500 W H₂/Air device, under specific design constraints, is reported.

The relative reactive fluid dynamics investigations indicated that the hydrogen-air solution does not present significant drawbacks in terms of combustion stability and efficiency.

In addition, [2] reports a Fourier parametric analysis carried out to mimic the device’s performance when works adopting only solar energy (mentioned as the “solar mode operation”), in which the sun has been simulated defining an external radiation source at a fixed temperature.

The “solar mode” investigation has been carried out to understand the effects of the dimensions of the holes (the combustion chambers) on the converter’s thermal conductivity and, consequently, on the overall energy efficiency.

Results indicate that the converter thickness should not exceed 6 mm to obtain a thermal efficiency greater than 20% when in the “solar mode operation”; this has meant that combustion chambers must not exceed 3 mm of diameter (that is the holes must not be greater than 3 mm for an efficient energy conduction). Moreover, [2] reports that a five connected chambers configuration matches with the following additional design requirements: $T_{\text{peak emitting surface}} > 1000 \text{ K}$, $\Delta T_{\text{emitting surface}} < 100 \text{ K}$ and emitting surface of $30 \times 30 \text{ mm}$.

The present manuscript investigates the same device, reported in [2], with the same design requirements but fed with methane.

It is important to understand the effectiveness of methane feeding because it is much easier, and safer, to be managed than hydrogen, it is a green propellant and, further, it is widely used, both for civil and space applications.

The current reactive numerical simulations adopt stoichiometric conditions, 500 W of injected chemical power, detailed chemistry, the k-eps turbulence approach and the eddy-dissipation concept to couple chemistry and turbulence.

In particular, the detailed hydrocarbon GRIMech mechanism [5], 32 species and 177 reactions, is adopted to reproduce the internal combustion.

Simulations show that, to fulfill with the design requirements, in terms of dimensions and efficiency, it is mandatory to add hydrogen, to the methane fuel injection, and to increase the operating pressure, up to 10 atm. This is due to the methane chemical structure, stiffer than hydrogen, which requires actions to increase the residence time and/or to accelerate the reaction.

The paper is structured as follows: section 2 describes the converter, the operating and boundary conditions, section 3 describes the numerical modeling, while sections 4–5 report, respectively, the results and the conclusions.

2. Energy Converter, Operating and Boundary Conditions

The parallelepiped brick has overall dimensions equal to $30 \times 30 \times 6$ mm, with inside 5 connected swirling combustion chambers characterized by a diameter of 3 mm. The total volume available for combustion is about 1200 mm^3 and the relative distance, between 2 consecutive chambers, is 3 mm. Figure 1 shows the hybrid converter with 5 connected chambers, two fuel-air entrances and only one outlet duct. This geometrical configuration permits to increase the residence time throughout the chambers. The internal chamber walls are coupled with the parallelepiped block, in order to permit the combustion products to heat up the emitting surfaces and then to deliver thermal power to the environment through convection and radiation; the emissivity values are reported in Figure 1.

The integration, between the swirling chambers and the emitting converter, is under a pending patent [6].

The external walls are characterized by a convective coefficient $H = 12 \text{ W}/(\text{m}^2 \cdot \text{K})$, calculated at standard and rest conditions.

Internal chamber walls are thermally conductive, while inlet and exhaust ducts walls are adiabatic (to mimic an eventual insulating material). The parallelepiped element is modeled adopting the following material properties:

Density, $\rho = 3100 \text{ kg}/\text{m}^3$;

Specific heat at constant pressure, $C_p = 600 \text{ J}/(\text{kg} \cdot \text{K})$

Thermal conductivity, according to the polynomial reported in [7].

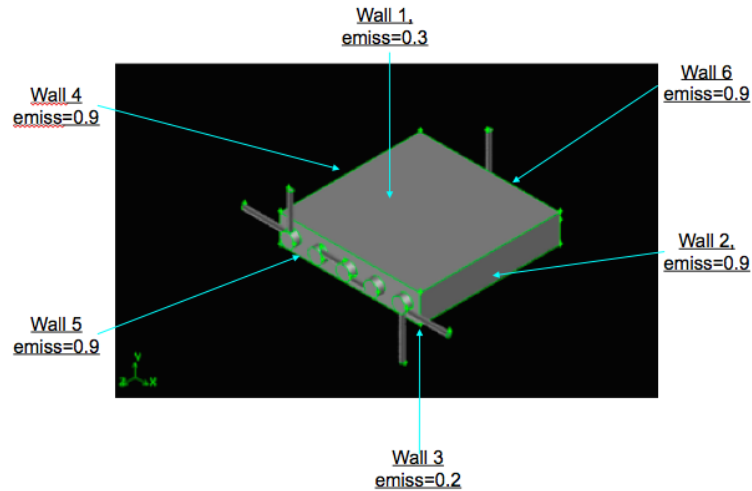


Figure 1. Swirling combustor converter, $Z/D = 11$, 5 connected chambers, emissivity values.

Table 1 reports the operating conditions of the 7 (seven) simulations.

Pure methane/air and hydrogen-methane/air blends, at different operating pressures, have been investigated. It is evident that laminar and moderately turbulent flow regimes are present, this is a typical feature of micro-meso/combustors [8,9]. Simulations were carried out assuming 500 W of injected power at stoichiometric conditions and adopting inlets temperature equal to 450 K, in order to mimic pre-heating at stationary conditions.

Table 1. Pure methane and methane-hydrogen blends, operating conditions.

H ₂ vol%	Pressure [atm]	Total injected chemical power (W)	Re (Fuel, Air)
		(CH ₄ -H ₂ /Air [kg])	
0	1	500 (1×10^{-5} -0/ 1.716×10^{-4})	430, 4415
20	1	500 (9.26×10^{-6} - 2.92×10^{-7} / 1.59×10^{-4})	390, 4100
50	1	500 (7.86×10^{-6} - 8.93×10^{-7} / 1.65×10^{-4})	365, 4350
20	5	500 (9.26×10^{-6} - 2.92×10^{-7} / 1.59×10^{-4})	390, 4100
50	5	500 (7.86×10^{-6} - 8.93×10^{-7} / 1.65×10^{-4})	365, 4350
20	10	500 (9.26×10^{-6} - 2.92×10^{-7} / 1.59×10^{-4})	390, 4100
50	10	500 (7.86×10^{-6} - 8.93×10^{-7} / 1.65×10^{-4})	365, 4350

3. Numerical Modeling

The domain has been reproduced by a mesh with a total number of cells greater than 1.4 M. The grid sensitivity analysis, reported in [1], indicated that a circumferential distance between gridpoints of 0.2 mm, on the chambers, and of 1 mm, on the walls of the brick, is the optimum. The grid analysis has been carried out at cold conditions because high temperature flows are characterized by smaller gradients (and then turbulence) than the ones at cold conditions with the same boundary conditions (Reynolds number decreases with the increase of the temperature).

The mesh has been improved by “reordering, smoothing, and swapping” techniques. In particular, reordering (the reverse Cuthill-McKee method [10]) was adopted to reduce the bandwidth of the cell neighbour number, in order to speed up the calculations, while “smoothing and swapping” were used, respectively, to reposition nodes (by lowering the maximum skewness of the grid) and to modify the cell connectivity and the relative overall quality.

The first point near the wall is at $y^+ < 3$ and $\Delta y^+ < 1$ (only a few points, in the air inlet ducts where velocities are higher, are close to $y^+ \sim 15$). This means that the first point away from the wall inside the chamber is within the viscous sublayer.

As mentioned in [8,9], in micro-meso combustors, laminar zones may co-exist locally with turbulent zones, therefore the laminar vs. turbulent regime uncertainty poses the problem of the modelling approach. A pure laminar approach would be unable to predict turbulent field zones, of crucial importance when reactions are present, while turbulent models would over-predict transport wherever the actual regime was laminar.

In the light of the above, fluid dynamics has been solved adopting the RANS k- ϵ s turbulence approach, with the enhanced wall treatment [11], able to reproduce accurate laminar dynamics [9].

The specific heat at constant pressure, $C_{p,i}$, is fitted by polynomials of temperature from the GRIMEch Thermo Data file [12], properly introduced in the CFD code, while viscosity and thermal conductivity, μ and k , are predicted by the gas kinetic theory [13]; mixtures are composition-dependent according to Wilke’s formula [14].

The turbulence-combustion coupling is modelled adopting the eddy dissipation concept (EDC) [15,16], while the methane/air kinetics by means of the GRIMEch mechanism [5], 32 species and 177 reactions.

The reactive Navier–Stokes equations were solved adopting a finite-volume solver (Ansys 14 CFD code). In particular, the pressure-based version, the PISO scheme [17,18] (for the pressure-velocity coupling) and the third-order MUSCL scheme [19] (for the spatial discretization of all the variables) have been implemented.

The computing resources are part of the CRESCO/ENEAGRID High Performance Computing infrastructure and its staff [20]. CRESCO/ENEAGRID High Performance Computing infrastructure is funded by ENEA, the Italian National Agency for New Technologies, Energy, and Sustainable Economic Development, and by Italian and European research programs [21].

4. Combustion Simulations Results and Discussion

The overall results are reported in the following Table 2.

It reports the combustion efficiency [Equation (1)], the average temperature at the exhaust section and the swirling number at reacting conditions calculated at $Z = 30$ mm. It is evident that the pure-methane feeding (additional H_2 equal to 0%) burns out. Therefore new strategies, to obtain stable combustion and efficient energy conversion, adopting hydrocarbon-air in such a small device, are mandatory. The chemical structure of the methane, sp^3 hybridized [22], affects the chemistry performance, requiring higher activation energy and longer residence time.

To this end, hydrogen has been added to the methane injection and the operating pressure has been increased; in particular six additional simulations have been carried out adopting a blend of 20% and 50%, in volume of hydrogen, and imposing an operating pressure of 1, 5 and 10 atm, see Table 1.

Combustion efficiency is defined as follow:

$$\eta_{\text{combustion}} = \frac{\chi_{CO_2}}{\chi_{CO_2} + \chi_{CO} + \chi_{UHC}} \Big|_{\text{outlet}} \quad (1)$$

Where $\chi_i = \frac{n_i}{n_{\text{tot}} - n_{H_2O}}$; and n_i is the molar fraction of species “i” at the exhaust section.

Table 2 indicates that, among all the simulations, only the ones with an operating pressure of 10 atm provide stable combustion, both with 20% and 50% in volume of additional hydrogen. The other configurations burn out.

Table 2. Overall results.

H ₂ vol%	Pressure [atm]	Combustion efficiency	Average Temperature at the exhaust section [K]	Swirling Number (reacting conditions)
0	1	Burns out	-	-
20	1	Burns out	-	-
50	1	Burns out	-	-
20	5	Burns out	-	-
50	5	Burns out	-	-
20	10	0.917	1433	1.615
50	10	0.982	1451	1.396

The figure 2 reports, as an example, the temperatures map on the xz plane, from which the extinction zones inside the two lateral chambers may be easily distinguished.

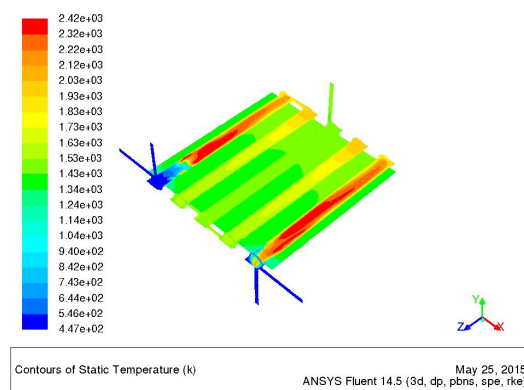


Figure 2. Temperature map, H₂ = 50%, P = 5 [atm].

Table 3 reports the maximum temperature, the minimum temperature, the average temperature, the standard deviation and, finally, the external heat transfer, respectively for “wall 1” and “wall 3” of the two configurations at 10 atm of operating pressure (respectively with H₂ = 20%–50% in volume of additional hydrogen).

The iterative solution was assumed converged when the difference between the inlet and outlet mass flow rates, $\Delta m/\Delta t$, was at least two orders of magnitude smaller than the smallest flow rate at the inlet section (that is, the hydrogen injection).

Table 3. $H_2 = 20\%$ and 50% vol, $P = 10$ atm, results.

H_2 % vol	External Heat Transfer Wall1–Wall3 [W]	Wall 1 $T_{\max}-T_{\min}$ [K]	Wall 1 $T_{\text{average}}-\sigma_T$ [K]	Wall 3 $T_{\max}-T_{\min}$ [K]	Wall 3 $T_{\text{average}}-\sigma_T$ [K]
20	70–51	1445–1304	1395–28	1446–1315	1397–28
50	73–53	1463–1334	1414–25	1462–1342	1416–25

The added hydrogen, being characterized by higher latent heat value and faster chemistry, than the methane, speeds up the overall reaction mechanism, while the increased pressure reduces the inlet velocities and increases the overall reaction rates.

These two strategies contribute, simultaneously, to increase the Damkohler number [23], defined as:

$$Da = \frac{\text{flow time scale}}{\text{chemical time scale}} \quad (2)$$

As expected, the configuration with $H_2 = 50\%$ in volume provides better performance in terms of combustion efficiency, maximum temperature and ΔT , on the emitting surfaces, than the one with additional $H_2 = 20\%$ in volume.

Notwithstanding, the overall outcomes are only slightly different, as the following discussion demonstrates.

Table 3 reports that the maximum temperatures, on both the emitting walls, are significantly greater than the design requirement ($T > 1450$ K vs. $T > 1000$ K). The total delivered power to the ambient is about 70 W–73 W, from “wall 1”, and 51 W–53 W, from “wall 3”.

Significant is the difference in combustion efficiency, $\eta_{H_2=50\%} > 0.98$ while $\eta_{H_2=20\%} > 0.91$, demonstrating how the faster hydrogen chemistry affects the final performance.

On the other hand the $\Delta T < 100$ K requirement is not fulfilled neither in the $H_2 = 20\%$ not in the $H_2 = 50\%$ configurations; in fact, the best result is $\Delta T \approx 120$ K, 20 K higher than the design requirement for the $H_2 = 50\%$ configuration. This value is confirmed also by the standard deviation value that is about 25 K versus 28 K in the $H_2 = 20\%$ configuration. This result would affect the overall performance in terms of compatibility with a thermo-photovoltaic cell, but only an experimental test would provide the concrete effects of such a ΔT .

The converter thermal behavior is shown in Figures 3–5, which present, respectively, the temperature maps of the combustion chambers walls, of the xz-plane and of the external walls.

In particular, Figure 4 shows that the maximum temperature, in the central core of the chambers, is around 2400 K for both the configurations.

Figure 5 reports the temperature maps of the emitting surfaces. It is evident that the low temperature zones, close to the inlet part of the converter, affect the overall performance, increasing the delta temperature, the standard deviation, and then lowering the eventual TPV energy conversion.

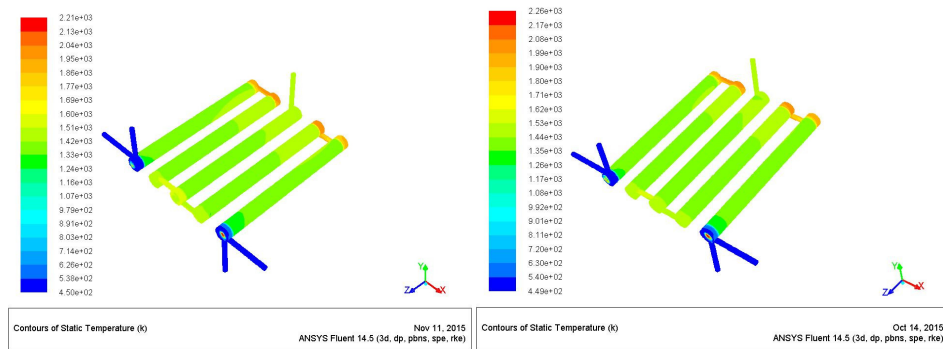


Figure 3. Temperature map of the five chambers, $H_2 = 20\%$ (left) and $H_2 = 50\%$ (right).

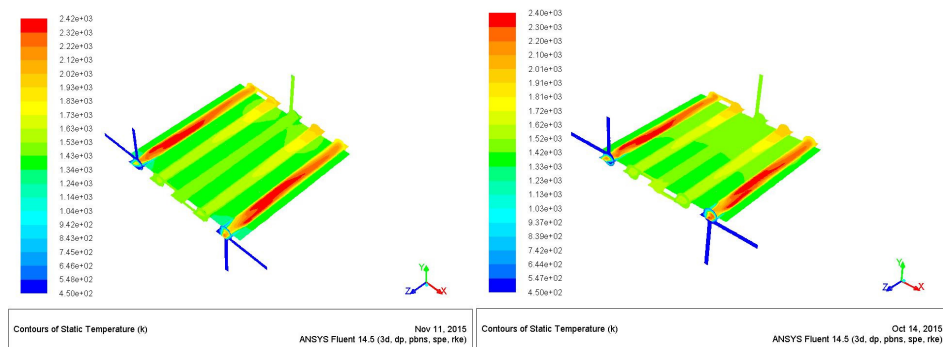


Figure 4. Temperature map on the xz-plane, $H_2 = 20\%$ (left) and $H_2 = 50\%$ (right).

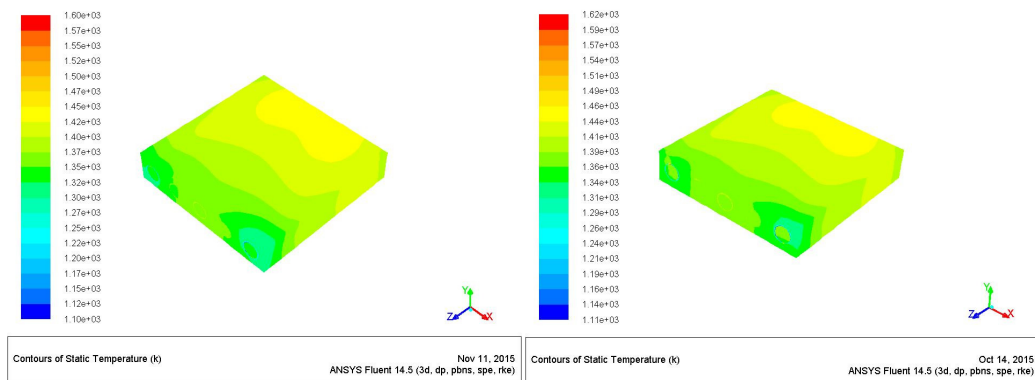


Figure 5. External walls temperature map, $H_2 = 20\%$ (left) and $H_2 = 50\%$ (right).

Finally, it is important to highlight the result regarding the average temperatures at the exhaust sections. The numerical investigations figure out 1433 K and 1451 K of exhaust temperature; this indicates that there is a lot of energy that might be still used, in both the configurations, to further increase the overall energy efficiency. To this end, the feasibility of connecting micro-turbine or micro-nozzle, for additional energy production or for space micro-propulsion, is under investigation.

Figure 6 reports, instead, the pressure maps inside the chambers; an overpressure of about 0.4–0.5 atm is present between the inlet and the outlet sections.

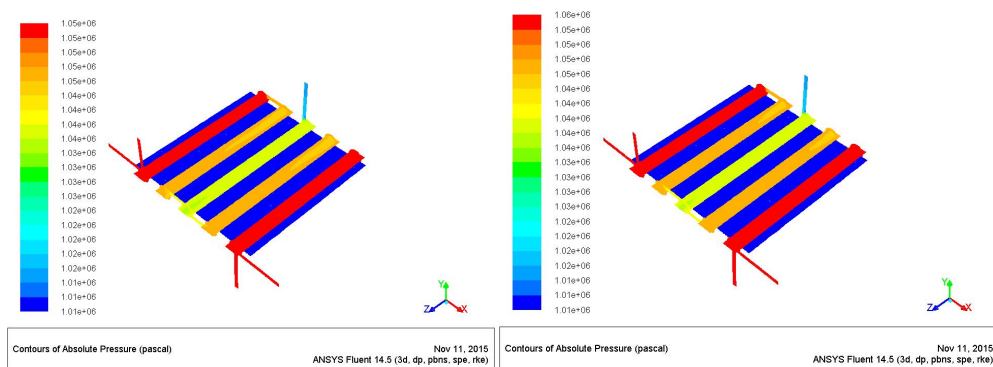


Figure 6. Pressure map, $H_2 = 20\%$ (left) and $H_2 = 50\%$ (right).

5. Conclusions

This work is the last development of a series of works, coming from an EU-FP7 project, that investigate the potentialities of an emitting parallelepiped block, with inside swirling chambers, as a hybrid energy converter connected to a TPV (hybridization considers to adopt solar energy and/or chemical energy).

The works in [1,2] investigated different configurations of a hydrogen-fed hybrid-converter, and in particular their effectiveness when compared to specific project's requirements.

The “solar mode investigations” imposed swirling combustion chambers of maximum 3 mm of diameter, while the combustion simulations showed no particular drawbacks or limitations when fed with hydrogen.

The present manuscript translated the previous outcomes to a hybrid-converter fed with hydrocarbons and the first result is the fact that methane is too stiff to maintain stable combustion inside the 3 mm-diameter connected swirling chambers; therefore, hydrogen has been added to the methane injection and the operating pressure has been increased up to 10 atm.

In particular, six simulations are carried out, adopting several hydrogen-methane blends ($H_2 = 20\%$ and $H_2 = 50\%$ in volume) and several operating pressure (1, 5 and 10 atm).

Among all the simulations, only the ones with 10 atm of operating pressure obtained successful results; all the other ones burn out.

The configuration with additional $H_2 = 50\%$ in volume performs, as expected, better in terms of combustion efficiency, maximum temperature and ΔT , than the one with $H_2 = 20\%$ in volume.

Both the configurations match with all the design requirements but miss the $\Delta T < 100$ K requirement. The best result is $\Delta T = 120$ K and it has been obtained adding $H_2 = 50\%$ in volume.

In the light of the above, only an experimental test could quantify whether, or not, this affects the TPV energy conversion performance.

The hydrogen addition and the pressure increase permit to reach high value of combustion efficiency ($\eta_{H_2=50\%} > 0.98$).

Moreover, a lot of energy is still available at the exhaust section of the converter.

This indicates that it is possible to increase the overall energy efficiency, for instance connecting the exhaust section with a microturbine or micronozzle in order to produce additional electrical energy or even thrust for microsatellite applications.

Acknowledgments

EU-FP7 ENERGY.2012.10.2.1: Future Emerging Technologies Grant, HRC Power Project.

Conflicts of Interest

The author declares no conflict of interest in this paper.

References

1. Minotti A, Teofilatto P (2015) Swirling combustors energy converter: H₂/Air simulations of separated chambers. *Energies* 8: 9930–9945.
2. Minotti A (2016) Energy converter with inside two, three, and five connected H₂/Air swirling combustor chambers: solar and combustion mode investigations. *Energies* 9: 461–475.
3. Harnessing Hybrids, Pan European Networks, 2013. Available from: <http://www.paneuropeannetworkpublications.com/st6/#/228/>.
4. Community Research and Development Information Service, 2013. Available from: <http://cordis.europa.eu/result/rcn/153340fr.html>.
5. GRI-Mech Version 1.2 released 11/16/94. Available from: http://www.me.berkley.edu/gri_mech/.
6. Minotti A, Ollier E. Hybrid energy converter based on swirling combustion and having a transversal heat path, FR 15 50448 (patent filed, 20/01/15).
7. Sui R, Prasianakis N, Mantzaras I, et al. (2016) An experimental and numerical investigation of the combustion and heat transfer characteristics of hydrogen-fueled catalytic microreactors. *Chem Eng Sci* 141: 214–230.
8. Minotti A, Sciubba E (2010) LES of a meso combustion chamber with a detailed chemistry model: comparison between the flamelet and EDM models. *Energies* 3: 1943–1959.
9. Minotti A, Cozzi F, Capelli F (2013) CH₄/Air mesocombustor at 3 bar: numerical simulation and experiments. *Appl Mech Mater* 431: 137–150.
10. Cuthill EH, McKee J (1969) Reducing bandwidth of sparse symmetric matrices. In Proceedings of the Association for Computing Machinery 24th National Conference, New York, NY, USA, 157–172.
11. Shih TH, Liou WW, Shabbir A, et al. (1995) A new k- ϵ eddy-viscosity model for high reynolds number turbulent flows. *Comput Fluids* 24: 227–238.
12. GRIMech 3.0 Thermodynamic Database. Available online: http://www.me.berkley.edu/gri_mech/version30/files30/thermo30.dat (accessed on 6 December 2015).
13. Anderson JD (1989) Hypersonic and High Temperature Gas Dynamics; McGraw Hill: New York, NY, USA, 12: 468–481.

14. Mathur C, Saxena SC (1966) Viscosity of polar gas mixture: Wilke's method. *Flow Turbul Combust* 15: 404–410.
15. Magnussen BF (1981) On the structure of turbulence and a generalized eddy dissipation concept for chemical reaction in turbulent flow. In Proceedings of the 19th American Institute of Aeronautics and Astronautics Aerospace Science Meeting, St. Louis, MO, USA, 12–15.
16. Gran IR, Magnussen BF (1996) A numerical study of a bluff-body stabilized diffusion flame. Part 2. Influence of combustion modelling and finite-rate chemistry. *Combust Sci Technol* 119: 191–217.
17. Issa RI (1986) Solution of implicitly discretized fluid flow equations by operator splitting. *J Comput Phys* 62: 40–65.
18. Ferziger JH, Peric M (1996) Computational methods for fluid dynamics. Springer-Verlag, Heidelberg, Germany.
19. Van Leer B (1979) Toward the ultimate conservative difference scheme V. A second order sequel to godunov's method. *J Comput Phys* 32: 101–136.
20. CRESCO: Centro computazionale di RicErca sui Sistemi Complessi. Available online: <http://www.cresco.enea.it/english> (accessed on 6 December 2015).
21. Ponti G, Palombi F, Abate D, et al. (2014) The role of medium size facilities in the HPC ecosystem: the case of the new CRESCO4 cluster integrated in the ENEAGRID infrastructure. In Proceedings of the 2014 International Conference on High Performance Computing and Simulation (HPCS 2014), Bologna, Italy, 1030–1033.
22. Silvestroni P (1992) Fondamenti di Chimica ED. IX, Masson-Veschi, 52–55.
23. Fogler S (2006). Elements of Chemical Reaction Engineering (4th ED.). Upper Saddle River, NJ: Pearson Education. ISBN0-13-047394-4.



AIMS Press

© 2017 Angelo Minotti, licensee AIMS Press. This is an open access article distributed under the terms of the Creative Commons Attribution License (<http://creativecommons.org/licenses/by/4.0>)